

Theoretical Analysis of Longitudinal-type Leaky Surface Acoustic Wave on LiNbO₃ with Oriented ScAlN Film

配向性 ScAlN 薄膜装荷 LiNbO₃ 上での縦型リーキーSAW の理論解析

Masashi Suzuki[†], Masashi Gomi, and Shoji Kakio (Univ. of Yamanashi)

鈴木 雅視[†], 五味 将史, 垣尾省司 (山梨大院)

1. Introduction

Surface acoustic wave (SAW) devices with high frequency operation are required for applications to RF filters in next generation mobile communications. Longitudinal-type leaky SAW (LLSAW) mode, whose phase velocity is approximately twice as high as that of other SAW modes, is suitable for high frequency SAW devices. However, the LLSAW possesses large attenuations because of the radiation of the bulk wave into substrate during the propagation. This causes low Q factor in SAW devices.

The authors demonstrated theoretically and experimentally that loading the amorphous AlN films with high velocity on the piezoelectric single crystal substrate leads the reduction of the attenuation in LLSAWs¹. However, the decreases of coupling factor K^2 were also observed in the LLSAW devices. This low K^2 is due to the non-piezoelectricity of the amorphous AlN films. We expect that the attenuation in LLSAWs will be reduced without the decrease of K^2 by loading the films with high velocity and high piezoelectricity on the piezoelectric substrate.

In 2009, Akiyama et al. reported the enhancement of piezoelectricity in Sc doped AlN film². The electromechanical coupling k_t in Sc_{0.41}Al_{0.57}N film bulk acoustic resonators is approximately 190 % of pure AlN film resonators.

In this study, the phase velocity, attenuation and K^2 for LLSAW in layered structure consisting of (0 θ ψ) Sc_{0.4}Al_{0.6}N film/X-cut 36°Y-propagation LiNbO₃ (X36°Y-LN) substrate were theoretically analyzed. From these propagation properties, the effect of the Euler angle and the film thickness of Sc_{0.4}Al_{0.6}N films on LN substrate were investigated.

2. Method for LLSAW theoretical analysis

Figure 1 shows the theoretical analysis model for LLSAW on the layered structure consisting of (0 θ ψ) Sc_{0.4}Al_{0.6}N film/ X36°Y-LN substrate. The propagation direction of the LLSAW was the x_1 direction. The phase velocity and the attenuation of the LLSAW were calculated by Farnell and Adler SAW propagation analysis method. The coupling factor K^2 were determined from $K^2 = 2 \cdot (v - v_{(si)or(ss)}) / v$, where v indicated the phase velocity in electrical free surface, $v_{(si)}$ or $v_{(ss)}$ is

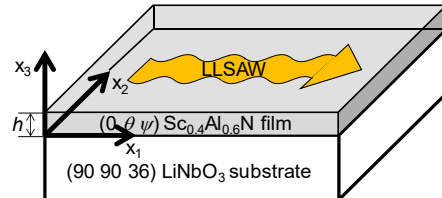


Fig.1 The theoretical analysis model for LLSAW propagation on air/Sc_{0.4}Al_{0.6}N film/LiNbO₃ substrate structure

the phase velocity in electric short interface or electric short film surface. The $v_{(si)}$ or $v_{(ss)}$ were used to determine K^2 of LLSAWs propagated on interface between ScAlN/LN or on ScAlN film surface, respectively.

3. Calculation result

The phase velocity in electric free surface v , as shown in **Fig. 2(a)**, were almost constant of approximately 7350 m/s without depending on Euler angle (0 θ ψ) and film thickness h/λ of Sc_{0.4}Al_{0.6}N films. As shown in **Fig. 2(d)**, the zero attenuations were obtained by loading (0 0 0) or (0 90 0) Sc_{0.4}Al_{0.6}N films in $h/\lambda > 0.02$. On the other hand, the attenuation in (0 90 90) Sc_{0.4}Al_{0.6}N film increased with increasing h/λ .

As shown in **Fig. 2(b)**, the phase velocity in electric short film surface v_{ss} increased for $0 < h/\lambda < 0.04$. The maximum values around $h/\lambda = 0.04$ of (0 0 0), (0 90 0) and (0 90 90) Sc_{0.4}Al_{0.6}N films were approximately 7500 m/s, 7400 m/s and 7200 m/s, respectively. The v_{ss} decreased with increasing the film thickness in $h/\lambda > 0.04$. As shown in **Fig. 2(e)**, the attenuations in (0 0 0) and (0 90 0) Sc_{0.4}Al_{0.6}N films were reduced to zero in $h/\lambda > 0.08$. In contrast, the zero attenuation was not observed in (0 90 90) Sc_{0.4}Al_{0.6}N film.

As shown in **Fig. 2(c)**, the phase velocity in electric short interface v_{si} of (0 0 0) or (0 90 0) Sc_{0.4}Al_{0.6}N films increased for $0 < h/\lambda < 0.05$. The maximum v_{si} around $h/\lambda = 0.05$ were approximately 7700 m/s. In $h/\lambda > 0.05$, the v_{si} decreased, and was close to 7350 m/s. The v_{si} of (0 90 90) Sc_{0.4}Al_{0.6}N film decreased for $0 < h/\lambda < 0.09$, and reached the minimum of 6600 m/s around $h/\lambda = 0.09$. The v_{si} increased in $h/\lambda > 0.09$. As shown in **Fig. 2(f)**, the attenuations of (0 0 0) or (0 90 0) Sc_{0.4}Al_{0.6}N films were zero in $h/\lambda > 0.08$ or $h/\lambda > 0.11$,

respectively. The attenuation in (0 90 90) $\text{Sc}_{0.4}\text{Al}_{0.6}\text{N}$ film increased with increasing h/λ , as with the electric free surface.

As shown in **Fig. 2 (g)**, a higher K^2 than LN plate was not observed in LLSAW propagated on $\text{Sc}_{0.4}\text{Al}_{0.6}\text{N}$ films surface. On the other hand, as shown in **Fig. 2 (h)**, the K^2 of LLSAW on interface between (0 90 90) $\text{Sc}_{0.4}\text{Al}_{0.6}\text{N}$ and LN was higher than that of LN plate. The maximum K^2 was 21% at $h/\lambda=0.09$, and is approximately 1.4 times higher than that of LN plate.

Finally, we investigated the effect of c-axis tilt angle θ in $\text{Sc}_{0.4}\text{Al}_{0.6}\text{N}$ film on the propagation properties of LLSAW on interface between ScAlN/LN . As shown in **Fig. 3 (c)**, the higher K^2 appeared in $80 < \text{c-axis tilt angle } \theta < 90$. On the other hand, as shown in **Figs. 3 (a) and (b)**, the zero

attenuations were not observed in these c-axis tilt angles. Unfortunately, at the present stage, we do not find the Euler angle and the film thickness of $\text{Sc}_{0.4}\text{Al}_{0.6}\text{N}$ film which satisfy both of low attenuation and high K^2 in LLSAW.

4. Conclusion

The effect of the load of (0 θ ψ) $\text{Sc}_{0.4}\text{Al}_{0.6}\text{N}$ films on X36°Y-LN substrates on LLAW propagation properties were investigated theoretically. When the LLSAW propagated on interface between (0 90 90) $\text{Sc}_{0.4}\text{Al}_{0.6}\text{N}$ and LN, the K^2 is higher than LN plate. However, the reduction of attenuation was not observed in these layered structures.

References

1. F. Matsukura and S. Kakio, Jpn. J. Appl. Phys., 53, 07KD04 (2014).
2. M. Akiyama et al., Adv. Mater., 21, 593 (2008).

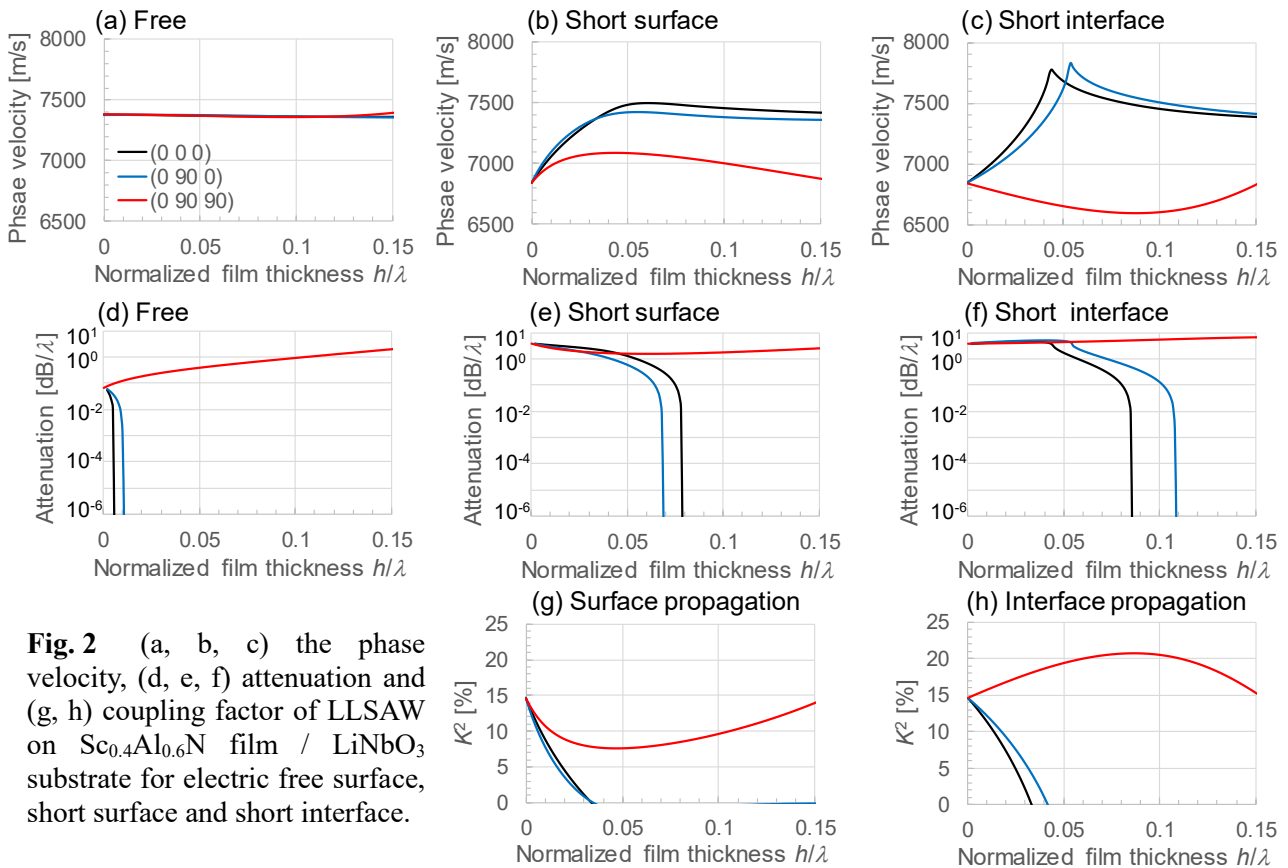


Fig. 2 (a, b, c) the phase velocity, (d, e, f) attenuation and (g, h) coupling factor of LLSAW on $\text{Sc}_{0.4}\text{Al}_{0.6}\text{N}$ film / LiNbO_3 substrate for electric free surface, short surface and short interface.

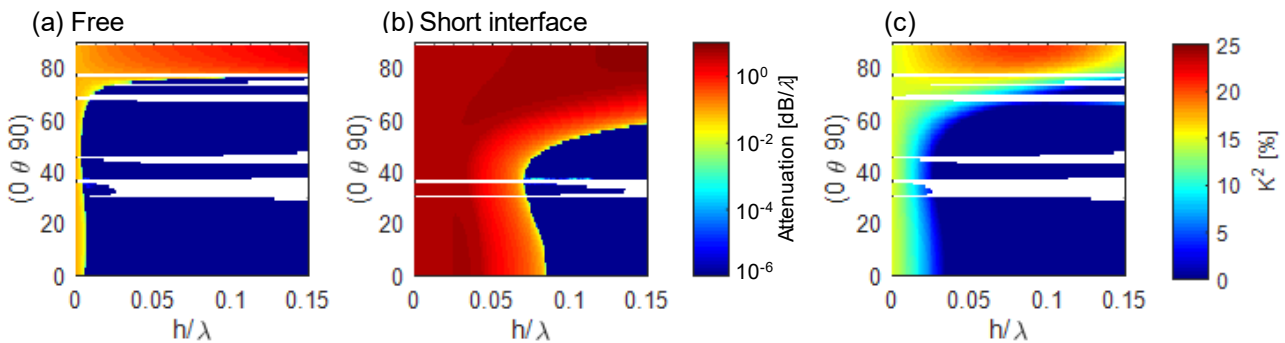


Fig. 3 The relationship between c-axis tilt angle in $\text{Sc}_{0.4}\text{Al}_{0.6}\text{N}$ film and (a, b) attenuation, and (c) coupling factor of LLSAW on interface of $\text{Sc}_{0.4}\text{Al}_{0.6}\text{N}$ / LiNbO_3 substrate.